Available online at www.sciencedirect.com
ScienceDirect
European Polymer Journal 42 (2006) 3311–3323
EUROPEAN POLYMER JOURNAL
www.elsevier.com/locate/europolj

# Cure kinetics of epoxy–amine resins used in the restoration of works of art from glass or ceramic

Evrikleia G. Karayannidou, Dimitris S. Achilias *, Irini D. Sideridou

*Laboratory of Organic Chemical Technology, Department of Chemistry, Aristotle University of Thessaloniki, GR- 541 24, Thessaloniki, Macedonia, Greece*

Received 8 May 2006; received in revised form 5 August 2006; accepted 31 August 2006
Available online 18 October 2006

**Abstract**

The cure kinetics of two epoxy/amine resins, Araldite 2020 and AY103-HY956 widely used as adhesives in the restoration of works of art from glass or ceramic was investigated using FTIR spectroscopy. These resins are two-part adhesives, consisting of a resin – A, based on a diglycidyl ether of bisphenol A, and a hardener – B which is either a cycloaliphatic amine (isophorone diamine) for Araldite 2020, or a mixture of three aliphatic amines in HY956. The study was based on the collection of IR spectra, in the middle range (4000–600 $cm^{-1}$), of mixtures of resin and hardener at different proportions and isothermal temperatures (22–70 °C) as a function of curing time. A kinetic model was employed to simulate the experimental data using two kinetic rate constants. Diffusion control was incorporated to describe the cure behaviour at high degrees of conversion. From fitting to experimental data the kinetic and diffusional parameters were estimated, together with the activation energies of the kinetic and autocatalytic rate constants. It was found that higher degrees of curing are obtained at higher temperatures and increased amounts of hardener. Differences in the performance of the two adhesives are explained based on the type of the amines used as hardener.


*Keywords:* Epoxy–amine resins; Cure kinetics; Restoration of works of art; FTIR; Kinetic modeling

## 1. Introduction

A good adhesive in order to be used for conservation and restoration of glass needs certain properties. It should be clear, colourless and with a refractive index close to that of glass, so that to become invisible in the glue line. Also it should retain this quality and should not discolour, shrink or embrittle upon ageing, as well as it should be strong enough to perform the job. In addition, it should not release any harmful volatiles upon curing or ageing, be easy to use, have a good shelf-life and be inexpensive. No adhesive can satisfy all these demands, since each one exhibits some advantages and disadvantages. Therefore, selecting a glass adhesive is a matter of compromise [1,2]. The adhesives used for glass repairs include polyurethanes, acrylic and cyanoacrylic esters, epoxy resins, silicones, polyesters etc. Epoxy resins generally are expensive, but the long service time and good

* Corresponding author. Tel.: +30 2310 997822; fax: +30 2310 997769.
*E-mail address:* axilias@chem.auth.gr (D.S. Achilias).

0014-3057/$ - see front matter © 2006 Elsevier Ltd. All rights reserved.
doi:10.1016/j.eurpolymj.2006.08.025

physical properties often help by providing a favourable cost-performance ratio when compared to other materials. Their advantages include curing at room temperature with low shrinkage, refractive index similar to that of glass and very high polarity. This last property is responsible for the formation of strong chemical bonds between the adhesive and the glass substrate. Epoxy resins are also used in conservation, for wood and stone consolidation and repair, consolidation of corrosion layer in metal, tear repair for paintings and as adhesives in ceramic conservation [3,4].

Among the epoxy resins specifically designed for glass bonding are Araldite 2020 (XW396/XW397) and Araldite AY103/HY956. Araldite is a Ciba-Geigy trade name, which is now owned by Huntsman Advanced Materials. They are two-part adhesives, consisting of a resin – A and a hardener – B that perform strong adhesion, curing at room temperature, extremely low shrinkage and resistance to humidity and mechanical stresses. The resin of both is based on a diglycidyl ether of bisphenol A (DGEBA), while the hardener is a cycloaliphatic amine (isophorone diamine) for Araldite 2020 and a mixture of different aliphatic amines in HY956. Araldite 2020 may also be used to bond metal, ceramics, rubber and rigid plastics and exhibits a refractive index similar to glass together with good chemical, heat and water resistance. Although these commercial products are extensively used, there is not any published paper dealing with their cure kinetics. The degree of curing as a function of time, as well as the time required for the complete cure is of great importance since it determines the time that is available for the application of the adhesive. Several parameters, such as temperature, hardener/epoxy ratio, type of amine or epoxy used, etc., affect cure kinetics. Therefore, the aim of this investigation is to study the kinetics of these epoxy resins at different reaction conditions.

Cure kinetics of epoxy resins have been studied experimentally with different techniques, such as Fourier transform infrared (FTIR) and Raman spectroscopy [5–11], gel permeation chromatography [12], thermal analysis as differential scanning calorimetry (DSC) [13–27], dielectric relaxation spectroscopy [28,29] and different approaches have been used to describe it. Using FTIR the evolution of the oxirane ring absorbance, at 915 $cm^{-1}$, is recorded in relation to a reference vibration band, whose intensity does not vary during the curing process. In contrast, indirect methods of analysis, like DSC, give only an assessment of the degree of cure by monitoring, as a function of time, the amount of heat released assuming that it is proportional to the rate of polymerization. Among these methods, FTIR spectroscopy represents the most attractive choice owing to the unmatched wealth of molecular level information contained in the infrared portion of the electromagnetic spectrum [5]. Furthermore, several models arising from proposed kinetic mechanisms have been used to fit the experimental data. Due to the complex chemistry involved in the epoxy curing, a phenomenological approach is the most popular for these systems. Besides classical kinetic expressions, phenomena such as autocatalysis in the early stages or the effect of diffusion on the kinetic rate constants at later stages can further complicate modelling. Development of a good kinetic model enables one to predict how the system will behave during cure and what the final degree of curing will be. Thus, the experimental work required to establish a cure cycle for any new conditions is minimized.

In this paper, cure kinetics of both Araldite 2020 and AY103/HY956 was investigated at different isothermal reaction temperatures (from 22 to 70 °C) and hardener/epoxy ratios using FTIR. A kinetic model was employed to simulate the experimental data and kinetic and diffusional parameters were estimated at all different conditions. The effect of the different type of hardener used in these resins (i.e., cycloaliphatic or a mixture of aliphatics) on the cure kinetics (i.e., autocatalytic or *n*th order) is also illustrated.

## 2. Experimental

### 2.1. Materials

Araldite® 2020 consists of two components A and B and it was supplied by Huntsman, Switzerland (Batch No. AD30940500). Component A, is a mixture of two epoxy resins, i.e., the diglycidyl ether of bisphenol A (DGEBA) (CAS No. 25068-38-6) with a number average molecular weight, $M_n < 700$ (corresponding to $n = 0$, or 1) (40–52% w/w) and the diglycidyl ether of 1,4-butanediol (DGEBOH) (CAS No. 2425-79-8) (50–62% w/w) as reactive diluent. Component B, the hardener, consists of a cycloaliphatic amine, the isophorone diamine (IPDA). The chemical structure of the epoxy compounds and amine used appear in Fig. 1. The epoxide equivalent weight (EEW) of component A, defined as the grams of resin containing 1 gmol

**Araldite 2020**

Component A. Epoxy resins

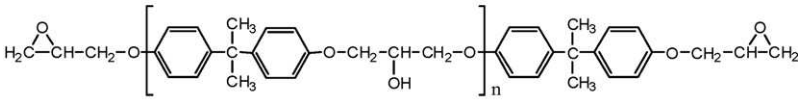

Diglycidyl ether of bisphenol A – DGEBA

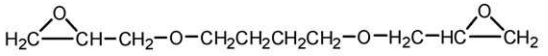

Diglycidyl ether of 1,4 butanediol (DGEBOH)

Component B. Hardener

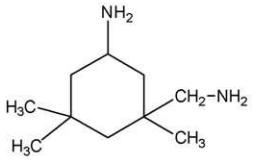

Isophorone diamine (IPDA)

**Araldite AY103/HY 956**

Component A. epoxy resin

DGEBA containing the plasticizer dibutyl ester of 1,2-benzenedicarboxylic acid

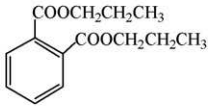

Component B. amines

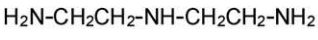

Diethylene triamine (DETA)

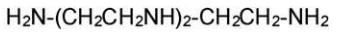

Triethylene tetramine (TETA)

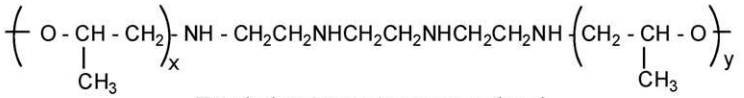

Triethylenetetramine propoxylated

Fig. 1. Molecular structure of epoxy compounds and amines used.

of epoxy group, was determined by titration according to literature [30] and it was found equal to 224.29 g/eq. The amine hydrogen equivalent weight (AHEW) was calculated by using the following equation: AHEW = molecular weight of the amine/number of active amine hydrogens. The isophorone diamine with a molar mass of 170.3 g/mol contains four active hydrogen atoms and acts theoretically as a tetramine. Thus AHEW of isophorone diamine is equal to $170.3/4 = 42.57$ g/eq. Since it is assumed that one amine hydrogen reacts with one epoxy group the stoichiometric ratio of hardener to use with the epoxy resin is given by the ratio: AHEW $\times$ 100/EEW of resin or $42.57 \times 100/224.29 = 19$ phr (phr = parts by weight of amine per 100 parts of resin). The supplier of Araldite 2020 recommends the use of phr = 30 for this system. Therefore, the phr ratios used in the present work were 30, 25 and 20, which correspond to 58%, 25% and 5% excess of amine, respectively.

Araldite® AY103/HY956 consists also of two components A and B and it was supplied by Huntsman, Switzerland (Batch No. AD 40374400). Component A is again DGEBA containing the plasticizer dibutyl ester of 1,2-benzenedicarboxylic acid (16.7% w/w), while component B is a mixture of

three amines, i.e., diethylene triamine (DETA), triethylene tetramine (TETA) and propoxylated triethylene tetramine (Fig. 1). The epoxide equivalent weight (EEW) of component A was determined again by titration and it was found equal to 291.4 g/eq. The supplier of this adhesive recommends the use of phr = 18 for this system. The AHEW of the hardener was 52.45 g/eq.

### 2.2. Sample preparation

For each Araldite studied the appropriate amounts of the two components A (epoxy resin) and B (hardener) were completely mixed by stirring at room temperature until they formed a homogeneous mixture. From this solution, several samples were prepared by casting a thin film on a glass plate covered by a polyethylene film and followed by covering the sample with another glass-polyethylene plate. These sandwich-like glass plates were placed in a thermostated oven (TERMAKS, B8000 series, mod. B 8054) at several curing temperatures (22, 50 or 70 °C). At pre-specified time intervals, each glass plate was removed and the sandwich-like polyethylene plate was mounted in an FTIR spectrometer.

### 2.3. FTIR measurements

The FTIR spectra of the samples were recorded at room temperature immediately after the oven cure. Since very slow reaction rates were observed (reaction lasted for more than a day in some experiments) compared to the time of measurement (only a few seconds), no polymerization was assumed to occur during the measurement [23]. A different sample was used at each time interval. All the spectra were obtained at a resolution of 4 $cm^{-1}$ using a Perkin–Elmer Spectrum One, FTIR. The recorded wavenumber range was from 600 to 4000 $cm^{-1}$ and 16 scans were averaged to reduce the noise. A commercial software Spectrum v5.0.1 (Perkin Elmer LLC 1500F2429) was used to process and calculate all the data from the spectra. The sample (sandwich-like polyethylene plate) was taken out of the glass plate and placed on a NaCl pellet since KBr may act as a catalyst in the reaction.

The relative conversion ($\alpha$) of the epoxy groups denoting the degree of curing at any time, $t$, was calculated by the following equation:

$$\alpha = (C_0 - C_t)/C_0 = 1 - C_t/C_0 \quad (1)$$

or taking into account that the Beer-Lambert law holds, by the relation:

$$\alpha = 1 - \frac{(A_{epoxy}/A_{ref})_t}{(A_{epoxy}/A_{ref})_0} \quad (2)$$

where $C$ is the concentration and A the absorbance of the group; the subscripts 0 and $t$ denote zero and reaction time $t$, respectively; the subscripts epoxy and ref are used to denote the characteristic epoxy and reference peak, respectively. The reference peak used as an internal standard for the normalization of epoxy peak absorbance is that of *p*-phenylene group at 833 $cm^{-1}$. The analytical peak used for the epoxy group was that of oxirane ring deformation at 915 $cm^{-1}$. The peak area was used according to Ref. [6].

All the results presented in the following sections were taken from an average of at least three experiments.

## 3. Theoretical background

Kinetic modeling of the curing process, as in every polymerization reaction, can be approached in two ways: either mechanistic or semi-empirical [6]. The first approach is based on a detailed knowledge of the elementary reactions taking place during curing and in writing the rate equations for every single step. Accordingly population balances are derived for all chemical species present in the reactor, which constitute a set of simultaneous differential equations describing the time evolution of every component involved in the reaction. These equations are usually solved numerically provided that the appropriate rate constants of every elementary reaction are known. These are usually evaluated by fitting the simulation model to appropriate experimental data. This is a rather complicated process, which requires measurement of different properties changing during the reaction in order to provide a set of parameters having physical meaning. Not to mention the computational effort especially when side reactions together with diffusional phenomena play an important role in the process. The semi-empirical approach is a more straightforward method based on the identification only of characteristic functional groups reacting (i.e., epoxy group, etc.) and not on the individual species. Thus, simpler equations easily solved are obtained with a smaller number of parameters needed to be evaluated.

A simple, yet general set of equations describing epoxy–amine polymerization involves three main reactions and may be expressed as [31]:

(1) Primary amine addition

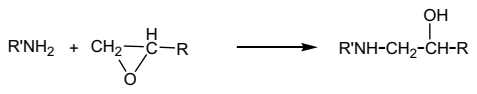


Primary amine Epoxide Secondary amine with hydroxyl group

(3)

(2) Secondary amine addition

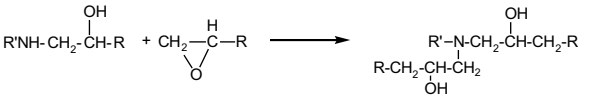


secondary amine epoxide Tertiary amine with hydroxyl groups

(4)

(3) Etherification reaction

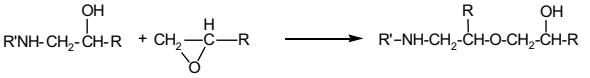


Secondary amine with ether and hydroxyl group

(5)

According to this kinetic scheme and with the simplifying assumptions of equal reactivity of primary and secondary amino-hydrogen with epoxy groups and a stoichiometric ratio of epoxy to amino-hydrogen groups, the following equation was obtained [13,18]:

$$\frac{d\alpha}{dt} = (k_1 + k_2\alpha)(1-\alpha)^2 \tag{6}$$

where $\alpha$ denotes conversion of the epoxy groups and the rate constants $k_1$ and $k_2$ correspond, respectively, to catalysis by groups initially present in the resin and catalysis by hydroxyl groups newly formed in the reaction. These rate constants depend on temperature with an Arrhenius-type expression:

$$k_i = A_i \exp(-E_i/RT) \tag{7}$$

where $A_i$ denotes the frequency factor of the $k_i$ rate constant and $E_i$ its corresponding activation energy.

If the epoxy and amine functional groups are not initially present in stoichiometric quantities then Eq. (6) is transformed to the following [13,32,33]:

$$\frac{d\alpha}{dt} = (k_1 + k_2\alpha)(1-\alpha)(B-\alpha) \tag{8}$$

where $B$ is the ratio of primary amine N–H bonds to epoxide functional groups in the initial mixture.

Furthermore, Kamal et al. [34,35] extended the so-called autocatalytic model using two additional empirical power law exponents $m$ and $n$ in addition to the kinetic rate constants $k_1$ and $k_2$. Thus Eq. (6) becomes:

$$\frac{d\alpha}{dt} = (k_1 + k_2\alpha^m)(1-\alpha)^n \tag{9}$$

This equation takes into account the autocatalytic nature of the curing process with the term $k_2\alpha^m$, while the $n$th order uncatalyzed process is represented by $k_1$. Eq. (6) can be derived from Eq. (9) using the values $m = 1$ and $n = 2$.

Many workers proposed different values of the empirical reaction orders $m$ and $n$, which were found to vary significantly with temperature [23,25]. Cole [36] recently developed a more rigorous model describing the cure kinetics of general epoxy–amine systems. He concluded that the reaction could be divided into two stages. At the beginning of the cure, the amine–epoxide reaction dominates and the effect of the etherification reaction is insignificant, so Eq. (8) is valid for the initial reaction. But in the later stages of curing, the isothermal cross-lining reaction tends to become simply first order with respect to epoxide concentration.

Eq. (9) was extensively used in literature and describes well the experimental data when epoxy conversion is completed (final degree of curing approaching 100%). However, when the epoxy resins polymerize at temperatures below the glass transition temperature of the polymer being formed, the curing reaction does not reach complete conversion. As the conversion increases and the $T_g$ of the mixture approaches the reaction temperature, the diffusivity of the reactive functional groups becomes seriously restricted. Thus, the curing reaction decreases considerably even when there may be a significant level of amino and epoxide groups available for reaction. Hence, a limiting conversion is usually achieved which is increased with the polymerization temperature. Kenny and coworkers [37], accounted for this effect by replacing the term $(1-\alpha)$ in Eq. (9) by $(\alpha_{max} - \alpha)$, with $\alpha_{max}$ representing the final conversion reached at the specified temperature. Thus. Eq. (9) is transformed to:

$$\frac{d\alpha}{dt} = (k_1 + k_2\alpha^m)(\alpha_{max} - \alpha)^n \tag{10}$$

Several authors used more fundamental approaches to model the effect of diffusion control on the polymerization kinetics [18,38]. Accordingly the overall kinetic rate constant $k$ is expressed in terms of a reaction-limited term $k_{chem}$ and a diffusion-limited one $k_{diff}$ [15,18].

$$\frac{1}{k} = \frac{1}{k_{chem}} + \frac{1}{k_{diff}} \Rightarrow \frac{k}{k_{chem}} = \frac{1}{1 + k_{chem}/k_{diff}} \tag{11}$$

the model proposed by Cook et al. [18] while more theoretically correct, it requires the determination of the change of the glass transition temperature as a function of curing conversion, which is not always known. In contrast, Chern and Poehlein [38] proposed a very simple equation coming from the free volume theory to estimate the ratio of the diffusion-controlled to reaction limited rate constant:

$$\frac{k_{\text{diff}}}{k_{\text{chem}}} = \exp(-C(\alpha - \alpha_c)) \tag{12}$$

where $C$ is a constant that depends on the structure, system and curing temperature and $\alpha_c$ is a critical conversion.

Thus the effective kinetic rate constants can be calculated using Eqs. (11) and (12) [15,36]. For values of $\alpha$ significantly lower than $\alpha_c$ the term $k_{\text{chem}}/k_{\text{diff}}$ is approximately equal to zero and $k/k_{\text{chem}} \cong 1$. This means that diffusion-controlled is negligible and the overall reaction kinetic rate constants are reaction-limited. When $\alpha$ approaches $\alpha_c$, $k/k_{\text{chem}}$ begins to decrease, reaching 0.5 when $\alpha = \alpha_c$. Beyond this point it continuous to decrease eventually approaching zero, so that the reaction becomes very slow and effectively stops. Therefore, $\alpha_c$ seems to correspond to a critical conversion above which vitrification is efficient, i.e., the vitrification conversion.

Later on Fournier et al. [28] modified Cole's equation as follows:

$$\frac{k}{k_{\text{chem}}} = \frac{2}{1 + \exp[(\alpha - \alpha_f)/b]} - 1 \tag{13}$$

with $\alpha_f$ denoting the final degree of curing and b a constant.

A comparison of the results obtained using Eqs. (11) and (12) with those from Eq. (13) and arbitrarily chosen values for the parameters $\alpha_c$, $C$ ($C = 22$, $\alpha_c = 0.64$) and $\alpha_f$, $b$ ($\alpha_f = 0.82$, $b = 0.09$) appears in Fig. 2. It is seen that both equations correspond to a gradual decrease with respect to degree of curing, while the Cole–Poehlein model presents also a gradual change during very high degree of $\alpha$. The Fournier et al. model presents monotonically decrease function with values of $k/k_{\text{chem}}$ less than zero when $\alpha > \alpha_f$.

From the aforementioned models and trying to keep the model adjustable parameters as few as possible, in this investigation we used the simple Horie Eq. (8) together with the diffusion model of Cole-Poehlein (Eqs. (11) and (12)). Thus, the final equation used can be written as [24]:

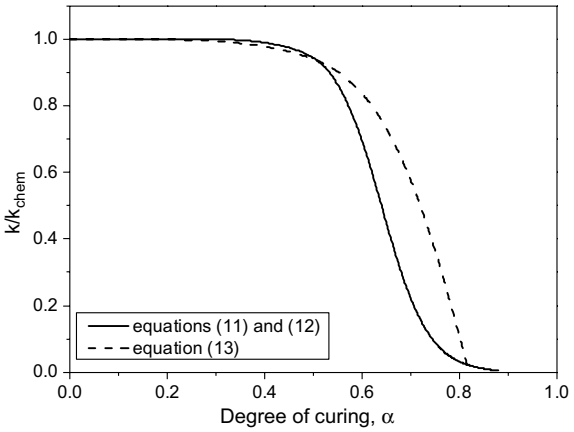


Fig. 2. Effect of the equation used to describe diffusion-controlled phenomena on the change of kinetic rate constants, as a function of the degree of curing during the epoxy–amine curing reaction.

$$\frac{d\alpha}{dt} = (k_1 + k_2\alpha)(1 - \alpha)(B - \alpha)\frac{1}{1 + \exp(C(\alpha - \alpha_c))} \tag{14}$$

## 4. Results and discussion

### 4.1. Analysis of the IR spectra

Fig. 3a and b shows the FTIR spectrum of the Araldite® 2020 film before and after curing, respectively. Several peaks are identified in Fig. 3a assigned either to the epoxy resin or to the hardener. The most important of these peaks is that of the oxirane ring at 915 $cm^{-1}$. Absorption at 3369, 3298, and 3174 $cm^{-1}$ is due to stretching vibration of the primary amino group ($-NH_2$) on the hardener structure. This group shows also an absorption peak at 1608 $cm^{-1}$. The strong peak at 2920 $cm^{-1}$ is due to the stretching vibration of $-CH_2-$ groups. The ether groups on the DGEBA molecule is characterized by three absorption peaks at 1250, 1038 and 950 $cm^{-1}$. The strong band at 1250 $cm^{-1}$ is due to aromatic carbon–oxygen stretching, while the band at 1038 $cm^{-1}$ results from the aliphatic carbon–oxygen stretching ($-O-CH_2-$). Finally, the bands at 1510 $cm^{-1}$ and 833 $cm^{-1}$ can be assigned to *p*-phenylene groups, while that at 950 $cm^{-1}$ is due to the epoxy ether group. After the end of cure, the epoxide group and the primary amine peaks both decreased in size (Fig. 3b). On the contrary new absorptions appear were revealed around 3400 $cm^{-1}$ due to secondary amine (N–H) and

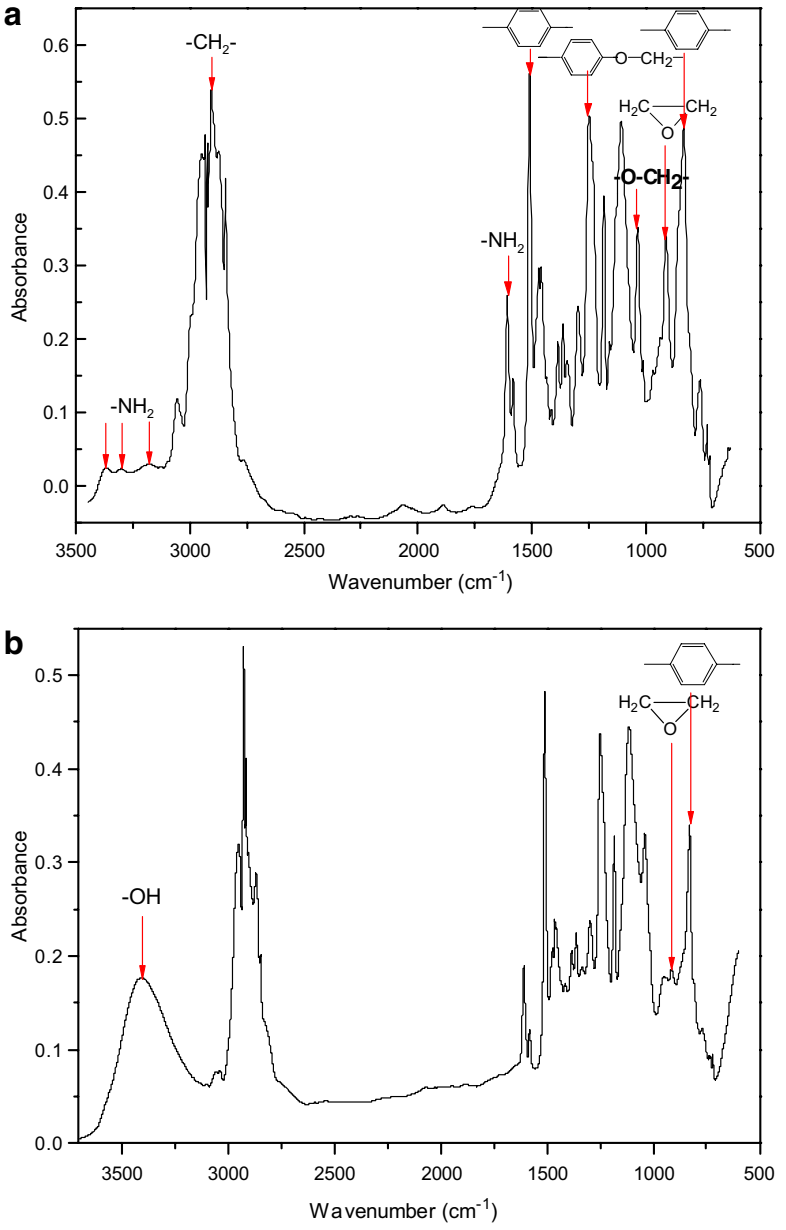


Fig. 3. FTIR spectrum, in the 3500–600 $cm^{-1}$ wavenumber range of Araldite 2020 thin film, before (a) and after curing (b).

hydroxyl groups formed during cure (Fig. 3b). The spectrum evolution of the Araldite® 2020 during curing at different times is illustrated in Fig. 4. A decrease in the area of the oxirane ring at 915 $cm^{-1}$ is obvious. It is also observed that the reference band of the *p*-phenylene groups at 833 $cm^{-1}$ and 1510 $cm^{-1}$ remain nearly constant throughout the treatment time. Repetitive experiments using either the peak at 833 $cm^{-1}$ or that at 1510 $cm^{-1}$ as a reference gave approximately the same results. Therefore, for quantitative measurements the band at 833 $cm^{-1}$ was used in this paper.

### 4.2. Evaluation of kinetic parameters

In order to evaluate the kinetic parameters appearing in Eq. (14) instead of estimating simultaneous four adjustable parameters, which perhaps would result in highly correlated values, the following procedure was followed. Initially the effect of

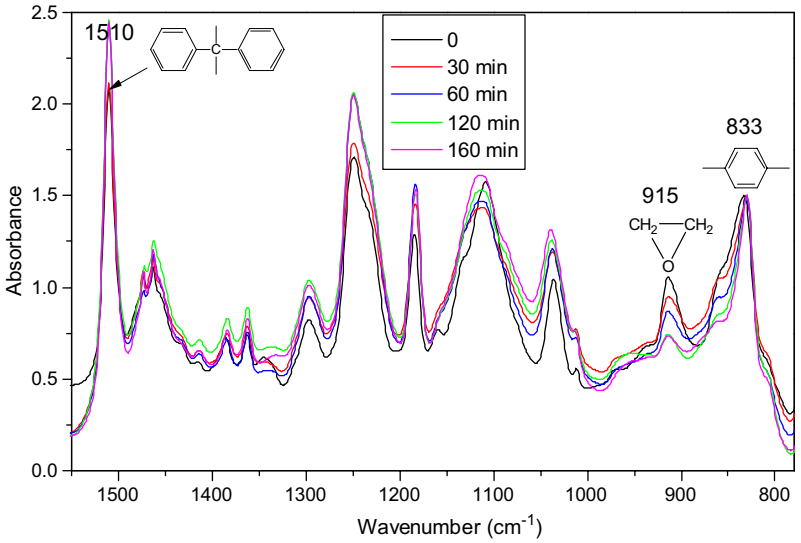


Fig. 4. FTIR spectra in the wavenumber range 1550–800 $cm^{-1}$ obtained at different times for the curing of Araldite 2020 at 70 °C; resin/hardener = 100/30 w/w.

diffusion-controlled phenomena was ignored. Thus, Eq. (8) could be integrated analytically to give:

$$C_1 \ln\left(\frac{k_1 + k_2\alpha}{k_1}\right) + C_2 \ln(1-\alpha) - C_3 \ln\left(\frac{B-\alpha}{B}\right) = t \tag{15}$$

with:

$$C_1 = \frac{k_2(1-B)}{(1-B)\left[k_1^2 + k_2^2 B + (1+B)k_1k_2\right]}$$

$$C_2 = \frac{k_1 + k_2 B}{(1-B)\left[k_1^2 + k_2^2 B + (1+B)k_1k_2\right]}$$

$$C_3 = \frac{k_1 + k_2}{(1-B)\left[k_1^2 + k_2^2 B + (1+B)k_1k_2\right]}$$

Eq. (15) provides an algebraic equation, which by means of some non-linear least-squares procedure, can be used to fit the experimental data of $\alpha$ as a function of time at different curing temperatures and amine/epoxy ratios. The best fitting values of the kinetic parameters $k_1$ and $k_2$ can then be estimated. Indicative results for the ratio of hardener to epoxy 20:100 wt/wt at 22 °C and 50 °C appear in Fig. 5. It was observed that the purely kinetic model fitted the experimental data very well at low conversions ($\alpha$ less than approximately 50%). However, the values measured at higher curing times were always overestimated. Thus, keeping the values of $k_1$ and $k_2$ estimated using low conversion data, the two diffusional parameters $C$ and $\alpha_c$ can be determined by fitting now the complete differential equation (14) to the experimental data. Using this procedure, the experimental data are simulated very well during the whole reaction time and the best set of adjustable parameters can be obtained.

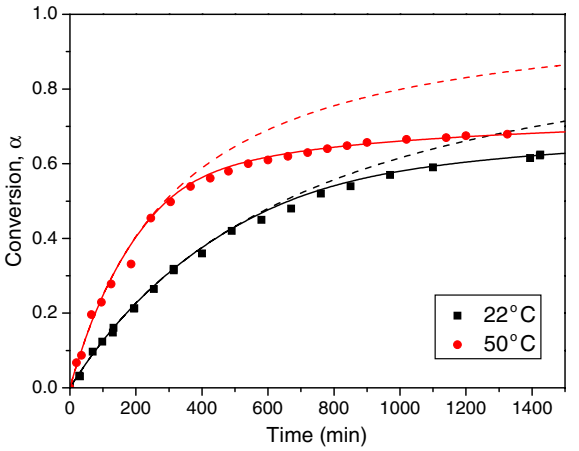


Fig. 5. Epoxy conversion versus time for the Araldite 2020 (phr = 30) at 22 °C and 50 °C. Solid lines were produced using Eq. (14), while dashed using Eq. (15) and omitting the effect of diffusion-controlled phenomena on the cure kinetics.

### 4.3. Kinetics of Araldite 2020

Fig. 6a, b and c show the effect of isothermal temperature on the conversion vs. time at three constant resin/hardener ratios 100:30, 100:25 and

100:20 w/w, respectively. It can be observed that conversion increases with time under given isothermal conditions and with temperature of isothermal cure. Initially the curing rate is high and later levels off resulting in a final degree of curing less than one in all experiments. The concentration of epoxy groups is not changed with further isothermal heating, although a number of residual epoxy groups remained un-reacted. This final degree of curing increases with temperature and is attributed to the effect of diffusion-controlled phenomena and the restricted mobility of the functional groups to come into close contact in order to react. At the 100:30 resin/hardener ratio (recommended by the supplier) after approximately 1 day of curing, the maximum epoxy conversion, $\alpha$, was approximately 74% at 22 °C, increased to 93% at 70 °C. The corresponding values measured at the almost stoichiometric ratio of resin/hardener (100:20 w/w) were 63% at 22 °C and 78% at 70 °C.

Furthermore, using the procedure described in Section 3.2 the best fitting values of the adjustable parameters were calculated and are illustrated in Table 1. Using these values differential Eq. (14) is integrated to provide the theoretical simulation curves of $\alpha$ as a function of time. The kinetic model results are also included in Fig. 6a, b and c as continuous lines. As it can be easily seen, the kinetic theoretical model simulates the experimental data very well at all different experimental conditions and during the whole evolution of conversion. From the values reported in Table 1, it can be seen that the estimated values of $C$ were unaffected by temperature. Concerning the variation of $C$ with temperature, no discernible trend was also observed in literature [15,16,24]. The estimated values range between 12 and 22 and are slightly lower than corresponding literature values (17–32 [16], 18–40 [24]). In contrast, the critical conversion, $\alpha_c$, was found to increase with temperature, again in accordance to literature data [15,16,24,39]. Since $\alpha_c$ corresponds to the vitrification conversion, i.e., conversion above which the effect of diffusion-controlled phenomena is important, it is expected that increased temperature increases the mobility of molecules and thus the onset of diffusion control may be shifted to higher values. Furthermore, it was interesting to compare these values with the gelation point (conversion at which a 3-dimensional network is formed). Theoretically, gelation occurs at a certain degree of cure that depends only on the functionality of the amine and epoxy. In the system examined, the amine is tetrafunctional and the epoxy is bifunctional so that the theoretical value

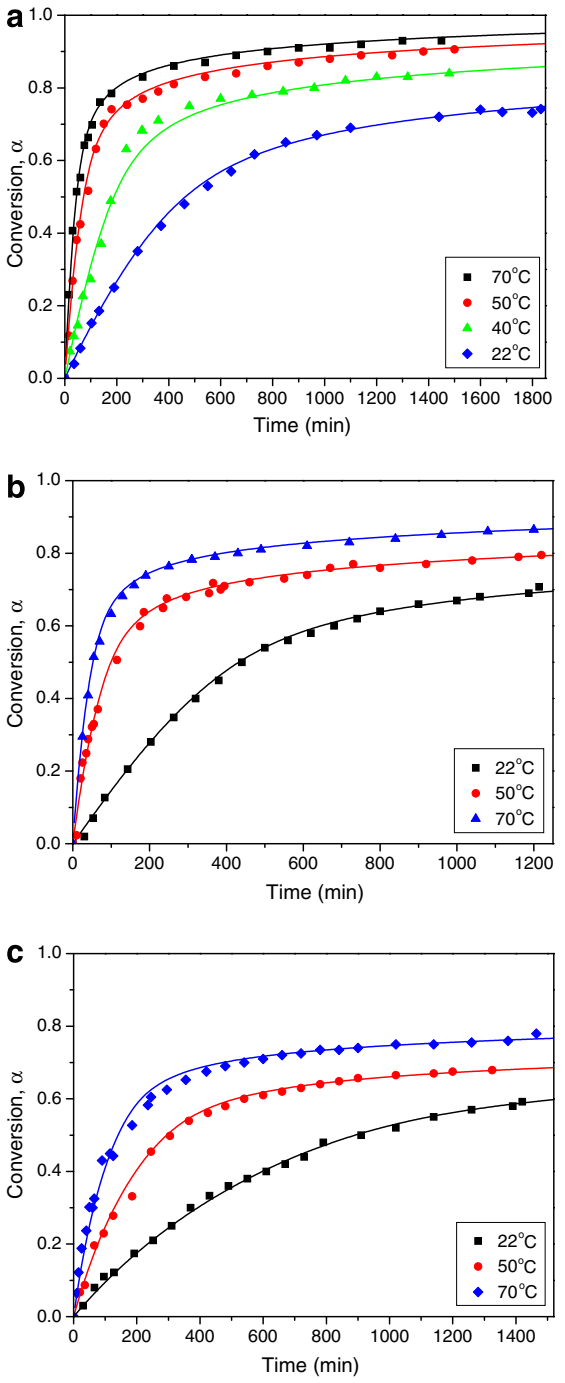


Fig. 6. Effect of isothermal temperature on the extent of conversion vs. time for Araldite 2020, cured at three constant resin/hardener ratios 100:30 (a), 100:25 (b) and 100:20 (c). Experimental data and kinetic model predictions.

Table 1
Kinetic and diffusional parameters at different temperatures and hardener/epoxy ratios of Araldite 2020

| Ratio of hardener to epoxy (wt/wt) | Ratio of amine equivalent to epoxy ($B$) | Temperature (°C) | $k_1 \times 10^3$ ($min^{-1}$) | $k_2 \times 10^3$ ($min^{-1}$) | $C$ | $\alpha_c$ |
|---|---|---|---|---|---|---|
| 30:100 | 1.58 | 22 | 0.95 | 1.0 | 12 | 0.61 |
| | | 40 | 2.2 | 2.7 | 12 | 0.66 |
| | | 50 | 6.4 | 4.5 | 12 | 0.68 |
| | | 70 | 10 | 8.0 | 12 | 0.69 |
| 25:100 | 1.25 | 22 | 1.2 | 2.0 | 15 | 0.60 |
| | | 50 | 6.5 | 4.0 | 15 | 0.60 |
| | | 70 | 12 | 7.5 | 15 | 0.66 |
| 20:100 | 1.05 | 22 | 0.98 | 0.3 | 22 | 0.58 |
| | | 50 | 3.0 | 0.8 | 22 | 0.58 |
| | | 70 | 6.0 | 2.2 | 22 | 0.64 |

of the extent of cure at gelation, $\alpha_{gel}$ for a stoichiometric amine/epoxy ratio should be [40]:

$$\alpha_{gel} = \left(\frac{1}{(f_A - 1)(f_E - 1)}\right)^{1/2} = \left(\frac{1}{(4-1)(2-1)}\right)^{1/2} = 0.577 \quad (16)$$

where $f_A$ and $f_E$ are the respective functionalities of the amine and epoxy.

Comparing this value (0.577) with those obtained for $\alpha_c$ in the near stoichiometric ratio ($B = 1.05$) and reported in Table 1, it is evident that $\alpha_{gel}$ is almost equal to $\alpha_c$ at low reaction temperatures (22 and 50 °C), whereas a higher $\alpha_c$ value was estimated at 70 °C.

Moreover, the values of the kinetic rate constants $k_1$ and $k_2$ are plotted as a function of temperature in an Arrhenius-type plot in Fig. 7a and b. The Activation energies, $E_1$ and $E_2$ calculated from the slopes of the straight lines, depend on the initial epoxy/amine ratio and are equal to: $E_1 = 43.4$, 41.1 and 31.8 kJ/mol and $E_2 = 36.8$, 28.3, 34.2 kJ/mol for $B = 1.58$, 1.25 and 1.05, respectively. It was observed that at high epoxy/amine ratios, the non-catalytic activation energy $E_1$, is greater than the autocatalytic, $E_2$, while at the almost stoichiometric ratio approximately equal values were obtained. It should be noted here that in literature both trends were reported (i.e., either $E_1 > E_2$, or $E_1 < E_2$) depending on the system and conditions examined. The $E_1$ and $E_2$ values estimated in this paper were slightly lower than corresponding literature values for different epoxy–amine systems (47.5 and 52.9 kJ/mol [23], 52 and 42 kJ/mol [18], 61.5 and 51.3 [7] and 61.2 and 47.7 [17]). Furthermore, Vyazovkin and Sbirrazzuoli in a series of papers

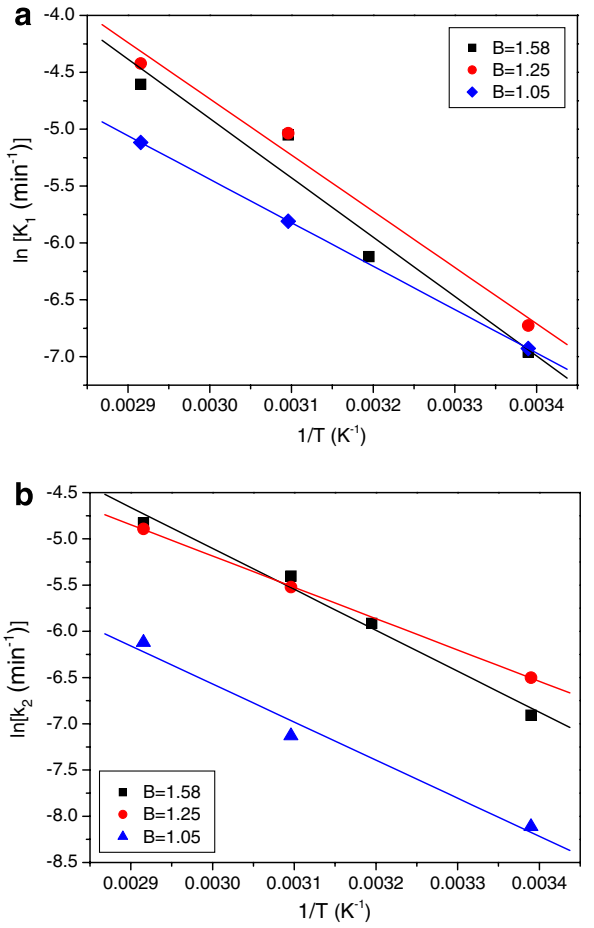


Fig. 7. Arrhenious-type plots of the kinetic rate constant $k_1$ (a) and the autocatalytic rate constant $k_2$ (b) as a function of temperature obtained from curing of Araldite 2020 at three initial amine/epoxy ratios, $B$.

[20,21,41,42] used the isoconversional kinetic analysis to study the kinetics of epoxy–amine systems.

The effect of viscosity on the kinetics of initial cure stages was also examined [42]. These authors, using an isoconversional approach for a similar epoxy–amine system estimated that the overall activation energy should be a function of the extent of cure and take values in the range of 30–45 kJ/mol [21]. According to isoconversional methods the reaction rate at constant extent of conversion is only a function of temperature. Therefore, the cornerstone of any isoconversional method is that one must have different experimental data at a constant extent of conversion. This can be easily carried out using an experimental technique, such as DSC where experimental data are recorded continuously. However, in such a technique like FTIR, used in this investigation, the experimental data are discrete and not continuously recorded. The IR spectrum is recorded at pre-specified time intervals which does not assure the measurement of the same extent of conversion at different experimental conditions. Therefore, by default the isoconversional analysis cannot be used in the experimental data of this manuscript.

Finally, Fig. 8 shows the effect of the resin/hardener ratio on the degree of epoxy conversion vs. time at a constant curing temperature. At each temperature studied it was observed that the initial conversion versus time data were almost the same at initial ratios of amine/epoxy equal to $B = 1.58$, or $B = 1.25$, while much smaller at the almost stoichiometric ratio of $B = 1.05$. The maximum degree of curing increased with the amine/epoxy ratio at high temperatures. These experimental observations are explained in terms of the kinetic model, since the values of the non-catalytic rate constant, $k_1$, which dominates initial the whole reaction, at $B = 1.58$ and 1.25 are approximately equal. Furthermore, $k_2$ which takes affect at higher conversion levels, is increased with the amine/epoxy ratio. It seems that higher content of hardener leads to more completed reaction of epoxy groups, resulting in a higher degree of epoxide consumption. This was also reported in literature for another epoxy/amine system [26]. Finally, increased ratio of hardener to epoxy results in lower values for the parameter $C$ and higher values for the critical conversion, $\alpha_c$.

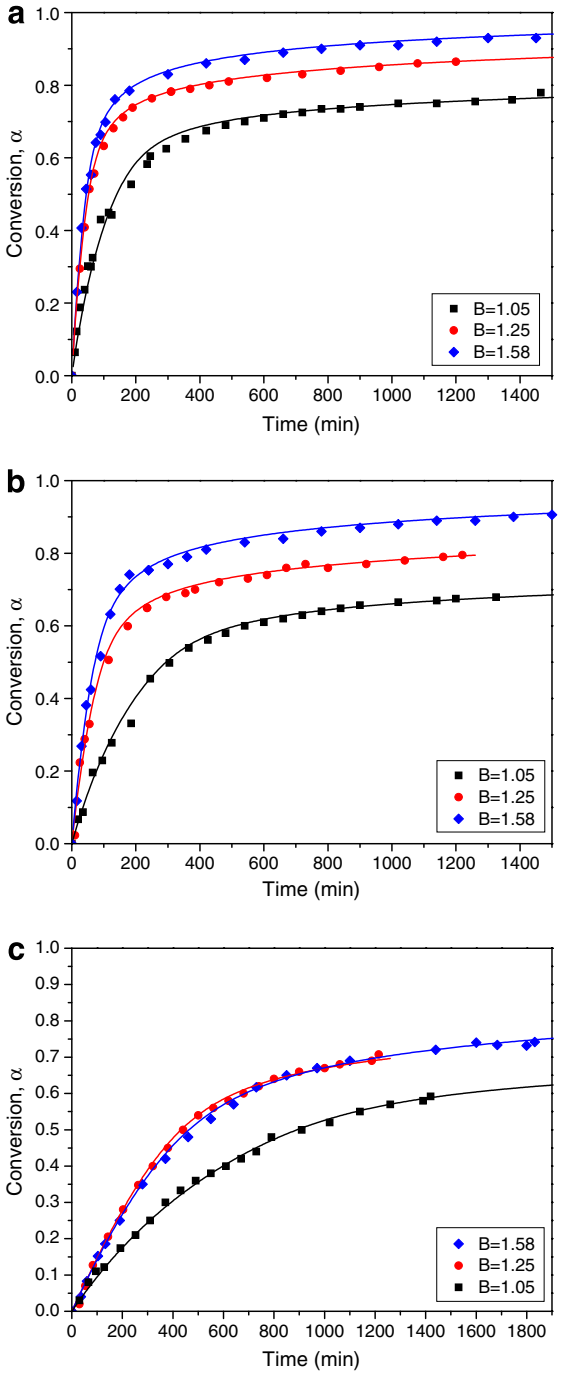


Fig. 8. Effect of the initial amine/epoxy ratio, $B$, on the extent of conversion vs. time for Araldite 2020, cured at three isothermal temperatures 70 °C (a), 50 °C (b) and 22 °C (c). Experimental data and kinetic model predictions.

### 4.4. Kinetics of Araldite AY103/HY956

Subsequently, the second Araldite epoxy/amine system was examined. The effect of isothermal temperature on the degree of curing versus time appears in Fig. 9. Again conversion increases with time with an initial high curing rate, which afterwards levels off resulting in a final degree of curing less than 1.

Again, using the procedure described in Section 3.2, the best fitting values of the adjustable parameters were estimated and are illustrated in Table 2. Using these values, the differential Eq. (14) is integrated to provide the theoretical simulation curves of $\alpha$ as a function of time. These lines are also included in Fig. 9 and results are compared to experimental data. Again, the theoretical kinetic model simulates the experimental data very well at all different experimental conditions. From the values reported in Table 2, it can be seen that the estimated values of $C$ were unaffected by temperature, while $\alpha_c$ increased with increasing temperature for the reasons explained in the previous section.

For this adhesive, even though the experimental data reported in Fig. 9, from a first glance resemble with those reported in Fig. 6 for Araldite 2020, from a closer look certain differences for this system were revealed. Initially, it was observed that conversion versus time data follow an *S*-shaped curve. This can be explained in terms of the kinetic model if the auto-catalytic kinetic rate constant, $k_2$, is much larger than $k_1$. Indeed, the values estimated for $k_2$ are nearly ten times those of $k_1$. Similar large differences with $k_2 \gg k_1$ have been also reported in literature for other epoxy/amine systems [16,25,27]. Furthermore, comparing the values of $k_1$ and $k_2$ obtained from both resins at corresponding conditions, it was observed that the values estimated for $k_1$ were very similar in contrast to $k_2$ where in Araldite AY103/HY956 the obtained values were more than ten times those of Araldite 2020. Therefore it was concluded that the mixture of aliphatic amines affects the autocatalytic part very much. From an Arrhenous-type plot of $k_1$ and $k_2$ versus temperature, the activation energies $E_1$ and $E_2$ can be determined from the slope of the straight lines (Fig. 10). Very good straight lines were obtained for both kinetic rate constants with a correlation coefficient, $R$, equal to 0.999. Then the values of the activation energies of the non-catalytic and autocatalytic kinetic rate constants were measured to be 51.8 and 47.3 kJ/mol, respectively. These values are close to those reported in literature for DGEBA/TETA 48.8 kJ/mol [43] or DGEBA/DETA 68.8 kJ/mol [44].

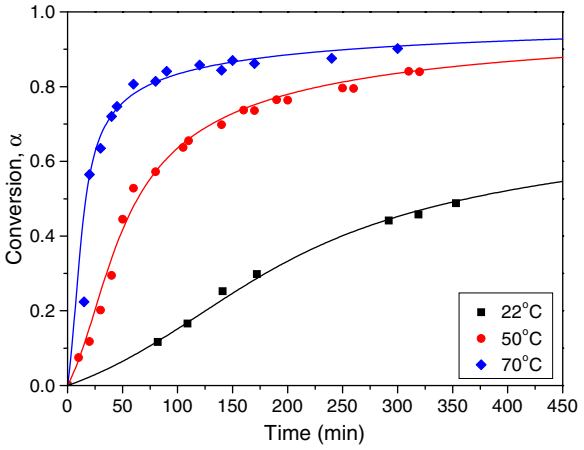


Fig. 9. Effect of isothermal temperature on the extent of conversion vs. time of Araldite AY103/HY956, cured at a constant resin/hardener ratios 100:18 w/w. Experimental data and kinetic model predictions.

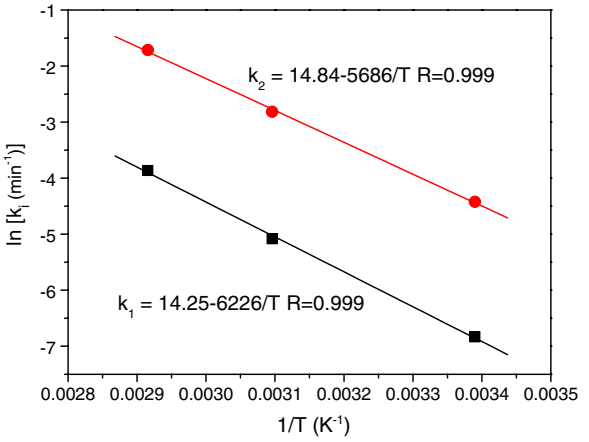


Fig. 10. Arrhenious-type plots of the kinetic rate constant $k_1$ and the autocatalytic rate constant $k_2$ as a function of temperature obtained from curing of Araldite AY103/HY956 at an initial resin/hardener ratios 100:18 w/w.

Table 2
Kinetic and diffusional parameters at different temperatures of Araldite AY103/HY 956

| Ratio of hardener to epoxy (wt/wt) | Temperature (°C) | $k_1 \times 10^3$ (min$^{-1}$) | $k_2 \times 10^3$ (min$^{-1}$) | $C$ | $\alpha_c$ |
|---|---|---|---|---|---|
| 18:100 | 22 | 1.08 | 12 | 8 | 0.43 |
| | 50 | 6.2 | 60 | 4 | 0.58 |
| | 70 | 21 | 180 | 8 | 0.65 |

## 5. Conclusions

In this study the cure kinetic of two epoxy/amine adhesives used in the restoration of works of art from glass or ceramic was investigated. These were Araldite 2020 and AY103/HY956 and the evolution of epoxy conversion with time was recorded using FTIR. The epoxy resin of both adhesives is based on DGEBA while the amine was a cycloaliphatic in the first case and a mixture of aliphatic in the second. Curing at room temperature is very slow process requiring more than a day to be completed, while curing at higher temperatures (up to 70 °C) leads to increased rates and final epoxy conversions. Furthermore, increased amounts of hardener with respect to resin also result in increased curing rates and final conversions. A kinetic model was employed accounting of both kinetic and diffusional limitations at high conversions and the parameters were evaluated by fitting to experimental data. Kinetics of both resins are very much affected by temperature and to a less extent by the amine/epoxy ratio, with increasing maximum degrees of curing with increasing amine. The mixture of aliphatic amines results in S-shaped conversion-time curves, which are due to larger values of the autocatalytic rate constant compared to the kinetic rate constant.

## References


[1] Davison S. Conservation and Restoration of Glass. 2nd ed. Oxford: Butterworth-Heinemann; 2003.
[2] Down JL. Review of CCI research on epoxy resin adhesives for glass conservation. Rev Conservat 2001;2:39–46.
[3] Horie CV. Materials for conservation – organic consolidants, adhesives and coatings. 8th ed. London: Architectural Press, an imprint of Butterworth-Heinemann; 1997.
[4] Selwitz C. Epoxy resins in stone conservation. Los Angeles: The Getty Conservation Institute; 1992.
[5] Mijovic J, Andjelic S. Polymer 1996;37:1295–303.
[6] Musto P, Martuscelli E, Ragosta G, Russo P, Villano P. J Appl Polym Sci 1999;74:532–40.
[7] Fraga F, Burgo S, Rodriguez Nunez E. J Appl Polym Sci 2001;82:3366–72.
[8] Bartolomeo P, Chailan JF, Vernet JL. Eur Polym J 2001;37:659–70.
[9] Eidelman N, Raghavan D, Forster AM, Amis EJ, karim A. Macromol Rapid Commun 2004;25:259–63.
[10] Escola MA, Moina CA, Nino Gomez AC, Ybarra GO. Polym Test 2005;24:572–5.
[11] Recalde IB, Recalde D, Garcia-Lopera R, Gomez CM. Eur Polym J 2005;41:2635–43.
[12] Mijovic J, Fishbain A, Wijaya J. Macromolecules 1992;25:979–85.
[13] Horie K, Hiura H, Sawada M, Mita I, Kambe H. J Polym Sci Part A1: Polym Chem 1970;8:1357–72.
[14] Moroni A, Mijovic J, Pearce E, Foun CC. J Appl polym Sci 1986;32:3761–73.
[15] Cole KC, Hechler JJ, Noel D. Macromolecules 1991;24:3098–110.
[16] Khanna U, Chanda M. J Appl Polym Sci 1993;49:319–29.
[17] Nunez L, Fraga Lopez F, Fraga Grueiro L, Rodriguez Anon JA. J Therm Anal 1996;47:743–50.
[18] Wise CW, Cook WD, Goodwin A. Polymer 1997;38:3251–61.
[19] Han S, Kim WG, Yoon HG, Moon TJ. J Polym Sci Part A: Polym Chem 1998;36:773–83.
[20] Vyazovkin S, Sbirrazzuoli N. Macromolecules 1996;29:1867–73.
[21] Vyazovkin S, Sbirrazzuoli N. Macromol Rapid Commun 2000;21:85–90.
[22] Nunez L, Fraga F, Fraga L, Castro A. J Appl Polym Sci 1997;63:635–41.
[23] Mezzenga R, Boogh L, Manson J-A, Petterson B. Macromolecules 2000;33:4373–9.
[24] Kim WG, Lee JY. J Appl Polym Sci 2002;86:1942–52.
[25] Rocks J, Halter M, George G, Vohwinkel F. Polym Int 2003;52:1749–57.
[26] Wu L, Hoa SV, Tan M, That T. J Appl Polym Sci 2005;99:580–8.
[27] Naffakh M, Dumon M, Dupuy J, Gerard J-F. J Appl Polym Sci 2005;96:660–72.
[28] Fournier J, Williams G, Duch Ch, Aldridge GA. Macromolecules 1996;29:7097–107.
[29] Pichaud S, Duteurtre X, Fit A, Stephan F, Maazouz A, Pascault JP. Polym Int 1999;48:1205–18.
[30] Sorenson RW, Campbell TW. Preparative methods of polymer chemistry. Interscience Publishers; 1961. p. 465.
[31] Prime RB. Thermosets. In: Turi EA, editor. Thermal Characterization of Polymeric Materials. New York: Academic Press; 1981.
[32] Sourour S, Kamal MR. Thermoch Acta 1976;14:41–59.
[33] Keny JM. J Appl Polym Sci 1994;51:761–4.
[34] Kamal MR. Polym Eng Sci 1974;14:231–9.
[35] Kamal MR, Sourour S. Polym Eng Sci 1973;13:59–64.
[36] Cole KC. Macromolecules 1991;24:3093–7.
[37] Keny JM, Apicella A, Nicolais L. Polym Eng Sci 1989;29:973–83.
[38] Chern CS, Poehlein GW. Polym Eng Sci 1987;27:788–95.
[39] Du S, Guo Z-S, Zhang B, Wu Z. Polym Int 2004;53:1343–7.
[40] Flory PD. Principles of Polymer Chemistry. Ithaca: Cornell University Press; 1953. p. 127.
[41] Sbirrazzuoli N, Vyazovkin S. Thermochim Acta 2002;388:289–98.
[42] Vyazovkin S, Sbirrazzuoli N. Macromol Chem Phys 2000;201:199–203.
[43] Mustata F, Bicu I. Polym Test 2001;20:533–8.
[44] Deng B, Hu Y, Chen L, Chiu W-Y, Wu T. J Appl Polym Sci 1999;74:229–37.